metals

MDPI

Article

Inconel 713C Coating by Cold Spray for Surface Enhancement of Inconel 718

Kaiqiang Wu [1,2], Sin Wei Chee [2], Wen Sun [1,2], Adrian Wei-Yee Tan [1,2,3], Sung Chyn Tan [4], Erjia Liu [1,2] and Wei Zhou [1,2,*]

[1] Rolls-Royce@NTU Corporate Laboratory, Nanyang Technological University, 65 Nanyang Drive, Singapore 637460, Singapore; kaiqiang001@e.ntu.edu.sg (K.W.); sunw0013@e.ntu.edu.sg (W.S.); adrian.tan@soton.ac.uk (A.W.-Y.T.); mejliu@ntu.edu.sg (E.L.)
[2] School of Mechanical and Aerospace Engineering, Nanyang Technological University, 50 Nanyang Avenue, Singapore 639798, Singapore; chee0138@e.ntu.edu.sg
[3] School of Engineering, University of Southampton Malaysia, Iskandar Puteri 79200, Johor, Malaysia
[4] Rolls-Royce Singapore Pte. Ltd., 1 Seletar Aerospace Crescent, Singapore 797575, Singapore; sungchyn.tan@rolls-royce.com
* Correspondence: mwzhou@ntu.edu.sg or wzhou@cantab.net; Tel.: +65-6790-4700

Abstract: Inconel 713C is a nickel-based superalloy usually considered as a material of poor weldability due to its susceptibility to hot cracking in the heat-affected zones. Cold spray, a solid-state deposition technology that does not involve melting, can be proposed as a methodology to deposit Inconel 713C for surface enhancement of other target components. In this study, Inconel 713C coating was deposited on Inconel 718 substrate with a high-pressure cold spray system. The coating was characterized in terms of microstructure, hardness, and wear properties. The cold-sprayed Inconel 713C coating has a low porosity level and refined grain structures. Microhardness of the Inconel 713C coating was much higher than the Inconel 718 substrate. The sliding wear tests showed that the wear resistance of the cold-sprayed Inconel 713C coating is three times higher than the Inconel 718 substrate, making the coating a suitable protective layer. The main wear mechanisms of the coating include oxidation, tribo-film formation, and adhesive wear.

Keywords: cold spray; additive manufacturing; Inconel 713C; Inconel 718; coating; wear; tribology

Citation: Wu, K.; Chee, S.W.; Sun, W.; Tan, A.W.-Y.; Tan, S.C.; Liu, E.; Zhou, W. Inconel 713C Coating by Cold Spray for Surface Enhancement of Inconel 718. *Metals* **2021**, *11*, 2048. https://doi.org/10.3390/met11122048

Academic Editors: Hamid Jahed and Guijun Bi

Received: 5 November 2021
Accepted: 16 December 2021
Published: 17 December 2021

1. Introduction

Inconel 713C is a nickel-based superalloy that possesses excellent creep resistance and oxidation resistance at high temperatures; thus, it is usually applied in jet engines, industrial turbines, and dies for casting or forging. With the rapid formation of oxide films on the surface at high temperatures, the components fabricated with Inconel 713C also possess good wear resistance for high-temperature applications [1]. However, Inconel 713C is considered non-weldable as cracks could occur due to the high solidification rate in the fusion zone and the low thermal conductivity of the alloy [2]. Successful welding can only be accomplished by electron beam with special considerations [3,4]. Consequently, Inconel 713C components are mostly manufactured by casting, and repair them is considered non-practical.

Cold spray is an emerging additive manufacturing technology that deposits particles onto substrate in the solid state. Particles are accelerated to supersonic speeds by high-pressure and high-temperature gas via a convergent/divergent nozzle. Upon impact of particles on a substrate surface, the thermal softening effect outweighs the strain-hardening effect due to the transformation of kinetic energy to thermal energy. Thus, both the particles and the substrate go through drastic plastic deformation, and metallurgical bonding could form in the deformed regions [5]. Because there is no melting or solidification involved in cold spray, deposition can be achieved much faster compared with other additive manufacturing technologies. Furthermore, compared with thermal spray, the particle

temperature in the cold spray process remains much lower than the melting temperature, so there is little oxidation or phase transformation in either coating or substrate [6]. All this makes cold spray promising for repair and surface enhancement in various industries. Therefore, cold spray can be proposed as a method to deposit Inconel 713C for surface enhancement of other materials [7]. Moreover, there are few published studies that report cold spray Inconel 713C or other nickel-based superalloys with γ' (Ni_3Al, Ni_3Ti) as the main strengthening phase.

Inconel 718 is the most widely used nickel-based superalloy due to its high strength and corrosion resistance. However, parts made of Inconel 718 can be degraded due to wear and corrosion. There has been published research about cold-sprayed coatings for repair and surface enhancement of Inconel 718. Singh et al. [8] studied the effects of substrate roughness and spray angle on deposition behaviors of Inconel 718 coatings on Inconel 718. The hardness of the coatings in that study ranged from 417 to 481 $HV_{0.3}$ and the porosity ranged from 0.40% to 0.92%. In the study by Ma et al. [9], the hardness of cold-sprayed Inconel 718 coating on Inconel 718 substrate was as high as ~600 $HV_{0.3}$ and the porosity was reduced to ~0.21% with helium as the propellant gas. Tribological properties of cold-sprayed Inconel 718 coating on Inconel 718 substrate were investigated by Sun et al. [10]. Though coating hardness was 86.9% higher than the substrate, the wear rate of the Inconel 718 coating was only 27.1% lower than the Inconel 718 substrate. In the present study, to improve the surface properties of Inconel 718, Inconel 713C coatings were deposited on Inconel 718 substrate via a high-pressure cold spray system. Microstructures, hardness, and tribological properties of the Inconel 713C coatings were then investigated.

2. Materials and Methods

Gas-atomized Inconel 713C powder with particle sizes ranging from 15 μm to 45 μm (Sandvik, Sweden) was used as the feedstock in the cold spray deposition process. The substrate used was Inconel 718 alloy (Haynes International, USA). Before the cold spray deposition, the substrate surfaces were ground with sandpaper and then cleaned with ethanol.

A high-pressure cold spray system (Impact Innovations GmbH, Germany) was used for the deposition. Nitrogen (N_2) was used as the propellant gas, which was preheated to 1000 °C and pressurized to 4.5 MPa. The De Laval nozzle of the system was held perpendicular to the substrate surfaces with a standoff distance of 30 mm from the nozzle exit. The nozzle transverse speed was 500 mm/s and the feed rate of the Inconel 713C powder was 33 g/min. A coating of around 300 μm in thickness was achieved with 10 layers of deposition.

The coated samples were cut vertically to the coating–substrate interface. Subsequently, they were mounted in epoxy and then ground and polished. Final polishing was conducted using a colloidal silica suspension (~0.25 μm particle size). Optical microscopy (OM, Zeiss Axioskop 2, USA) images of the Inconel 713C coating were taken and then investigated with the ImageJ software for porosity calculation in compliance with the standard ASTM E2109-01 [8]. Backscattered electron (BSE) mode images were taken under a field emission scanning electron microscope (FE-SEM, JEOL JSM-7600F, Japan) with a BSE detector. Electron backscattered diffraction (EBSD) analysis of the coating was carried out using FE-SEM (JEOL JSM-7800 prime, Japan) with an EBSD detector (Oxford Symmetry S2, UK). The step size of the EBSD scan was 0.1 μm. Morphology of the Inconel 713C feedstock powder was observed using SEM (JEOL JSM-5600LV, Japan). A cross-section image of the Inconel 713C particle was taken with a similar method for the coated samples.

Microhardness of the coating and substrate was measured using a Vickers hardness tester (Future-tech FM-300e, Japan) with a load of 500 g. For both the hardness of coating and substrate, indentations were implemented 50 μm and 250 μm away from the coating–substrate interface.

Dry sliding wear tests were conducted both on the Inconel 713C coating and Inconel 718 substrate by using a ball-on-disk microtribometer (CSM High Temperature Tribometer, Anton Paar, Switzerland) following the ASTM G99 standard [9]. Prior to the wear tests,

surfaces of the samples were ground and polished and then cleaned with ethanol. A hardened 100Cr6 steel counter ball with a hardness of 60–66 HRC was used to slide on the rotating coated samples along a circular path of 1.5 mm in radius for 20,000 laps. The total sliding distance was about 188 m. Wear tracks were measured by a surface profilometer (Talyscan 150, USA) with a conical diamond stylus of 4 µm in diameter to calculate wear volumes. Specific wear rates (w) were then calculated with the equation $w = V/FL$ in which V (mm^3) stands for the volume of wear track, F (N) stands for the normal load, and L (m) stands for the sliding distance [6,10]. Three measurements were taken and then averaged for the wear rates of both the coating and the substrate. The wear tracks were observed under the FE-SEM to investigate the wear mechanisms.

3. Results and Discussion

3.1. Microstructure Characterization

Figure 1a shows that the Inconel 713C feedstock powder has a near-spherical shape, but some particles are attached with numerous satellites, which could affect the particle acceleration and further lead to low deposition efficiency. Figure 1b is the BSE-SEM image of the cross-section of a single Inconel 713C particle, in which a dendritic microstructure can be observed.

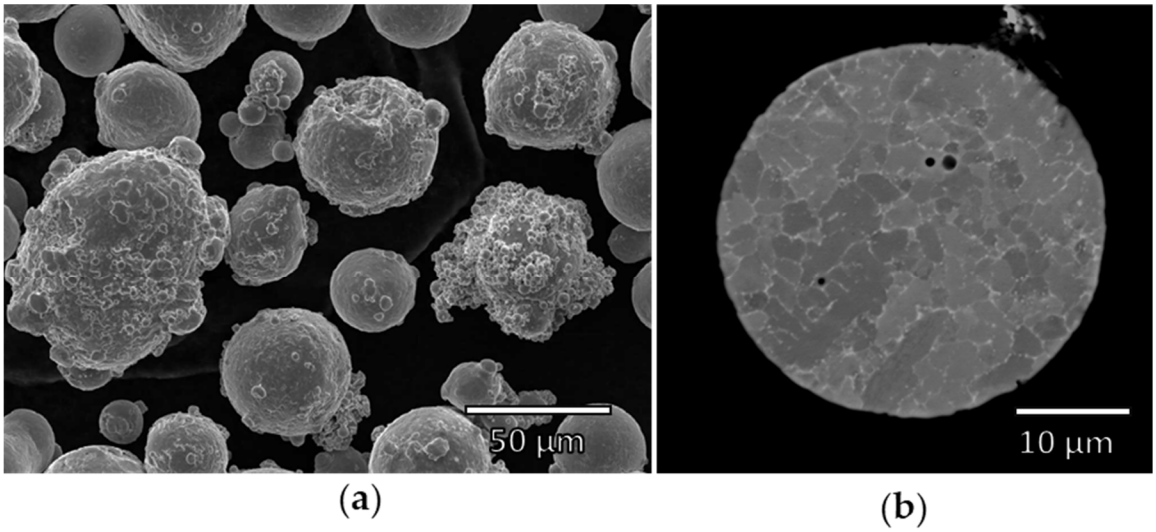

Figure 1. (**a**) SEM image of Inconel 713C feedstock powder. (**b**) BSE-SEM image of the cross-section of a single Inconel 713C particle.

Figure 2a is the optical image showing cross-section of the cold-sprayed Inconel 713C on Inconel 718. A dense coating microstructure is observed with a low porosity of ~1.23%. Because adiabatic shear instability (ASI) is triggered in the cold spray process, particles undergo severe plastic deformation upon impact. Jetting and splats formed during deformation tend to fill the voids and vacancies in the coating. The interface between the coating and the substrate is undulating and almost crack-free, indicating the deformation of the Inconel 718 substrate and strong adhesion between the coating and the substrate. With the deformation of both Inconel 713C particles and Inconel 718 substrate, metallurgical bonding could form at the interface [11].

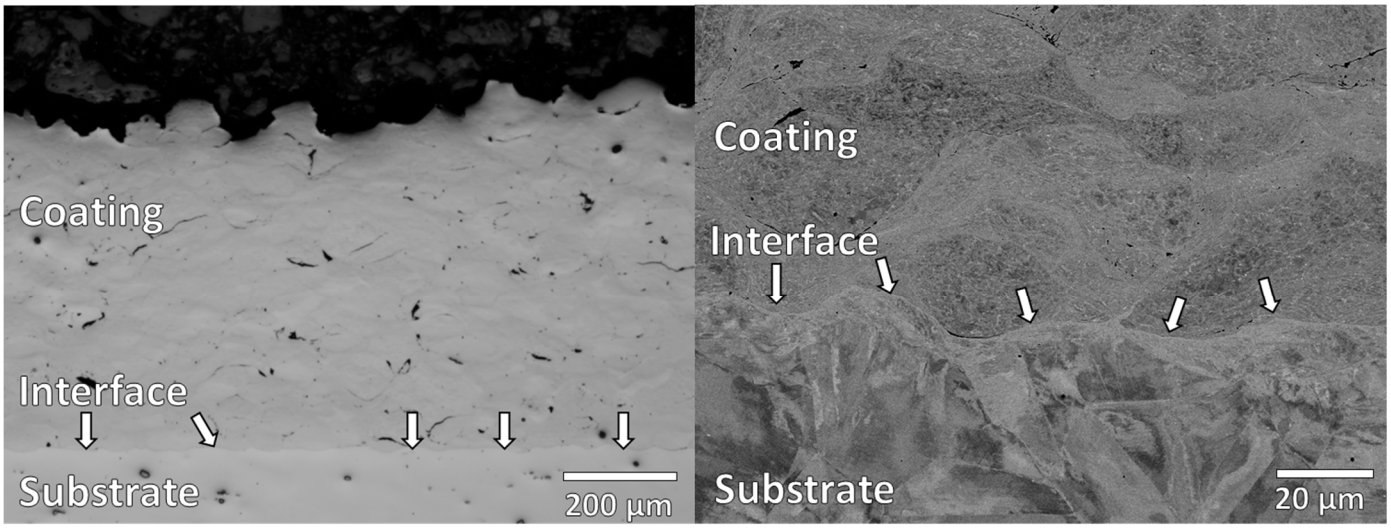

Figure 2. (**a**) OM image and (**b**) BSE-SEM images of the Inconel 713C coating on Inconel 718 substrate.

Figure 2b is the BSE-SEM image of higher magnification taken at the interface. The dendrite structure of the splats in the coating is heavily distorted compared with Figure 1b, which is also evidence of severe plastic deformation [12]. At the interface, some cracks can be observed, because metallurgical bonding usually forms at regions where jetting occurs [13]; other regions with poorer adhesion would appear as cracks in the BSE-SEM image. In the substrate, the microstructure in the region closer to the interface is distorted/refined compared to the region away from the interface, which can be attributed to the peening effect when Inconel 713C particles impact the Inconel 718 substrate.

Figure 3 demonstrates a detailed microstructure analysis of the Inconel 713C coating with EBSD scan. The BSE-SEM of the coating is shown in Figure 3a while the band contrast image, IPF, and Kernel average misorientation (KAM) map of the corresponding area are presented in Figure 3b–d, respectively. The band contrast and IPF mapping reveal that the coating microstructure contains fine grains, the size of which are considerably smaller than the original grains in the feedstock particles. Since the step size of the EBSD scan is 0.1 µm, grains that are smaller than the step size cannot be detected in the band contrast image (Figure 3b), leading to the unindexed black regions in the micrograph. As seen from the KAM map (Figure 3d), there is high dislocation density in almost all detected grains, which can be attributed to the high velocity impact of the particles during the cold spray process. The fine grain microstructure and inclusion of high dislocation density would have a significant influence on the hardness and tribological properties of the Inconel 713C coating, which will be discussed in the following sections.

3.2. Hardness

Figure 4 shows the hardness of the Inconel 713C coating and Inconel 718 substrate at different locations. The hardness of the coating is much higher than that of the substrate due to strain accumulation and finer grains in the coating. It can be seen from the error bar that fluctuation of the hardness values of the coating is larger than that of the substrate, which may be due to hardness indentation at the inter-particle boundaries with poor cohesive strength and pores that are randomly distributed in the coating [14].

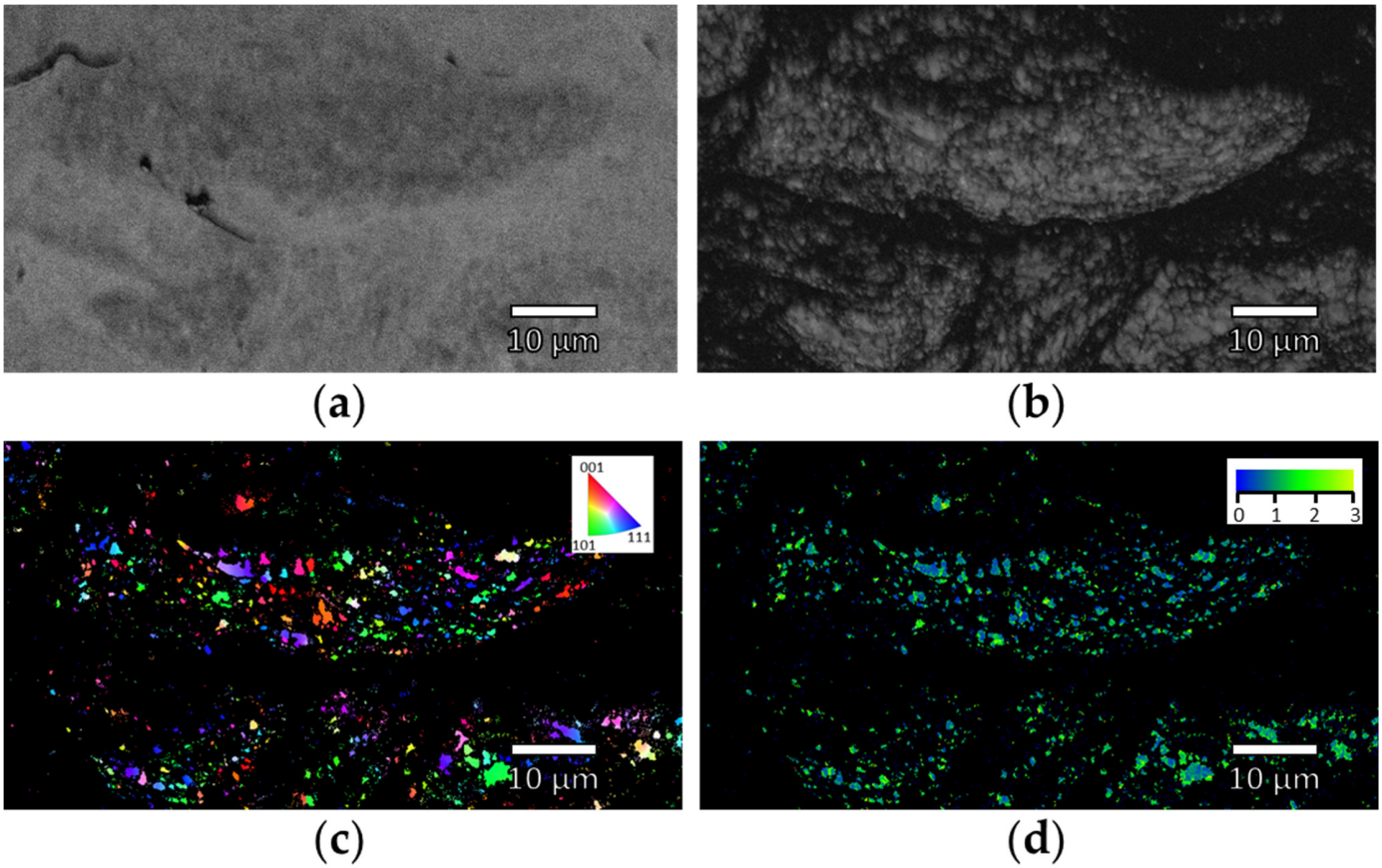

Figure 3. Microstructure analysis of the Inconel 713C coatings: (**a**) BSE-SEM image. EBSD images: (**b**) band contrast image showing grains, (**c**) IPF image showing grain orientations, and (**d**) Kernel average misorientation (KAM) map.

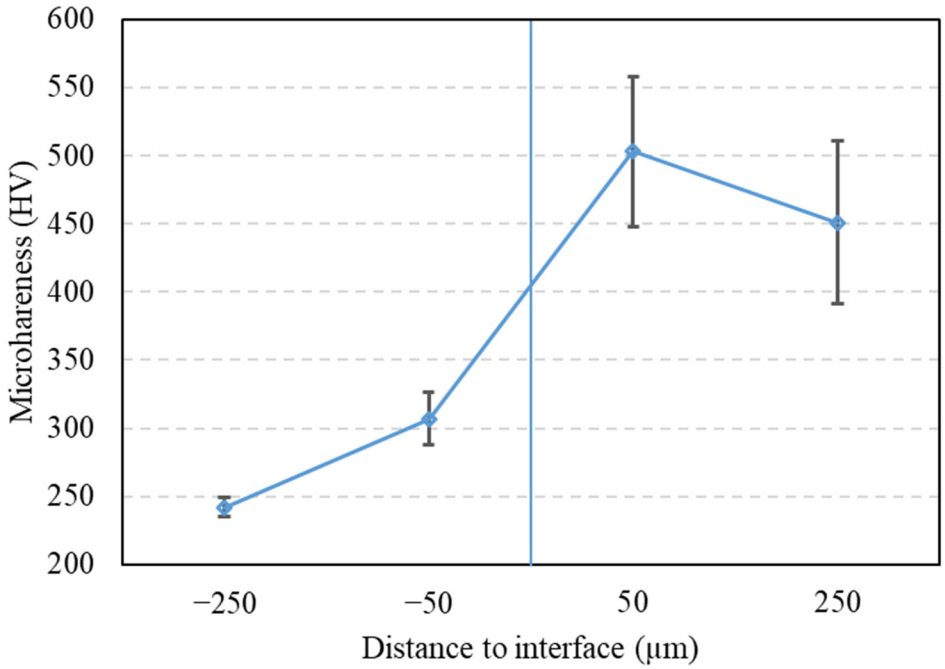

Figure 4. Microhardness of Inconel 713C coating and Inconel 718 substrate at different locations.

It is interesting to note that Vickers hardness values are higher (~500 HV) when the indentation was conducted at a short distance of 50 µm away from the interface compared with that further away at 250 µm (~450 HV). This may be attributed to the peening and

grain refinement effect from the Inconel 713C particles. In the substrate, regions close to the surface were shot peened and underwent grain refinement by the high-velocity particles; thus, hardness in those regions increased following the Hall–Petch relationship. The regions further away from the top surface were hardly affected.

The hardness variation of Inconel 713C coating is quite different from the results reported by Wu et al. [10], where consistent hardness values were observed at different locations of the cold-sprayed Inconel 625 coatings. This can be explained by the relatively low deposition efficiency of the Inconel 713C coating. With similar cold spray parameters, the deposition of the IN713C coating only achieved an efficiency of ~30 µm/layer while IN625 coating was ~80 µm/layer, almost 2.5 times more. Therefore, it can be hypothesized that rebounded Inconel 713C particles acted as "shot peening balls" to apply extra work hardening onto the deposited layer; hence, the bottom portion of the coating (50 µm to interface) received more peening or hammering and exhibits higher hardness [15]. Hardness is an indicator of wear resistance [16]; therefore, cold-sprayed Inconel 713C coating, with improved hardness compared with bulk Inconel 713C [17] and the Inconel 718 substrate, is promising to enhance the wear resistance of the Inconel 718 substrate.

3.3. Tribological Properties

The Inconel 713C coating is more wear resistant than the Inconel 718 substrate, as shown in Figure 5. The specific wear rate of the Inconel 718 substrate is three times that of the cold-sprayed Inconel 713C coating. As seen from Figure 6a, which is a representative image of the wear track of the Inconel 713C coating, the wear track is mostly covered by tribo-films, which can act as barrier to inhibit possible abrasive and adhesive wear during the sliding. In contrast, few tribo-films are observed on the wear track of the Inconel 718 substrate, as shown in Figure 6b, resulting in larger material removal caused by abrasive and adhesive wear. Tribo-films usually consist of metal oxides and can delaminate after repeated sliding. The fine grain structures of the Inconel 713C coating could promote the formation of metal oxides [18]; therefore, newly formed tribo-films would be sufficiently large and protective even though previous ones were delaminated or removed from the wear track due to centrifugal force. This also explains why the tribo-films covering the wear track of Inconel 713C coating can still be observed after the slide wear of 188 m.

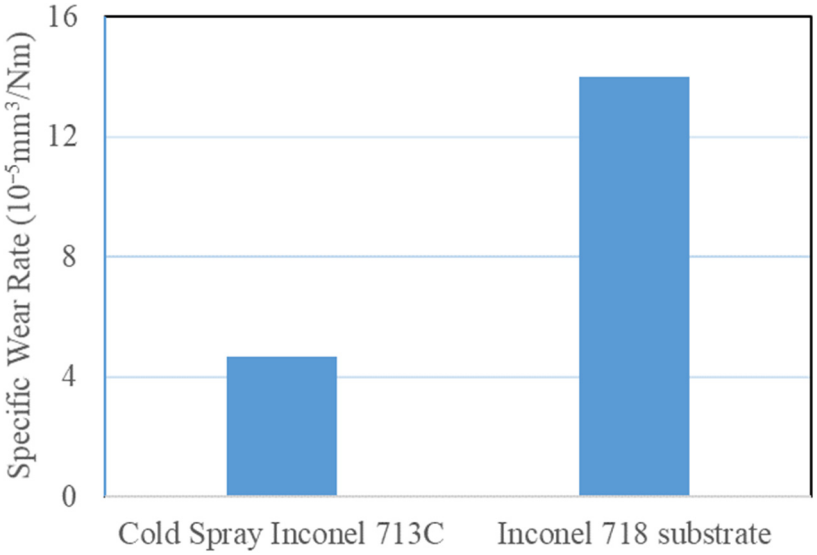

Figure 5. Specific wear rates of cold spray Inconel 713C coating and Inconel 718 substrate.

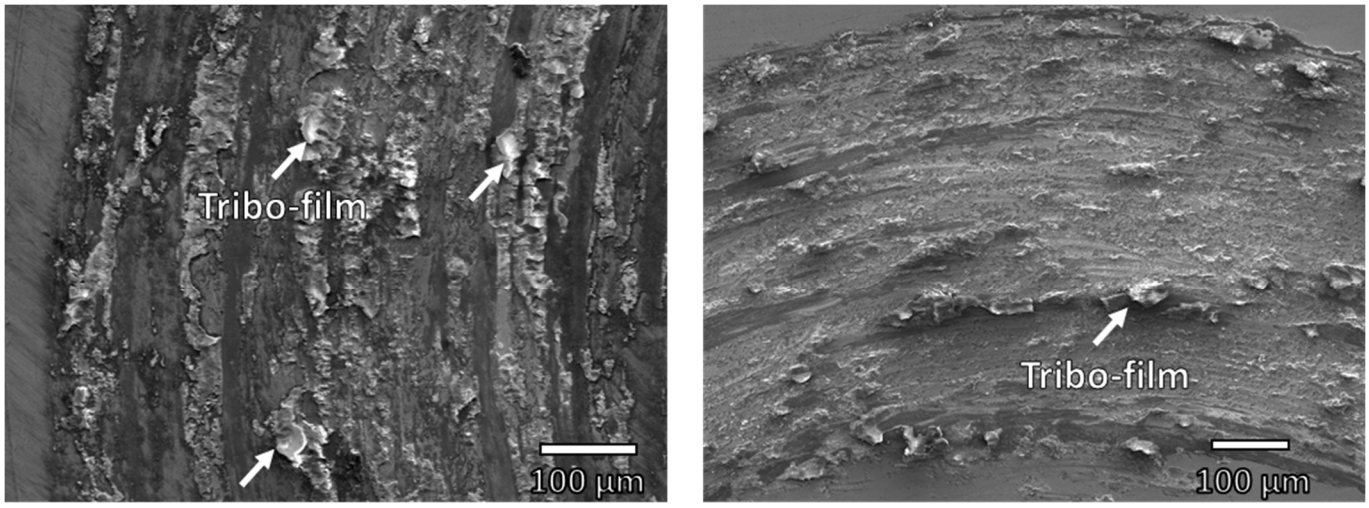

Figure 6. SEM micrographs of wear tracks of (**a**) cold spray Inconel 713C coating and (**b**) Inconel 718 substrate.

Another main wear mechanism for both the Inconel 713C coating and the Inconel 718 substrate is adhesive wear. Due to the adhesive force between the counter ball and the wear track, some material from the coating or substrate could be detached and transferred to the counter ball. The remaining material was deformed, leading to the unevenness of the wear tracks (Figure 7). Long shear bands in the shape of fish scales were discovered on the wear track of the Inconel 718 substrate (Figure 7b), while none exist on the wear track of the Inconel 713C coating. Since the hardness of the substrate is low, adhesion force could exceed the shear strength of the substrate and resulted in the excessive deformation where shear bands were formed [19]. The grooves (Figure 7) caused by abrasive wear [20] are scarce on wear tracks of both coating and substrate, but also due to lower hardness, more grooves are found on the Inconel 718 substrate as compared to those on the Inconel 713C coating.

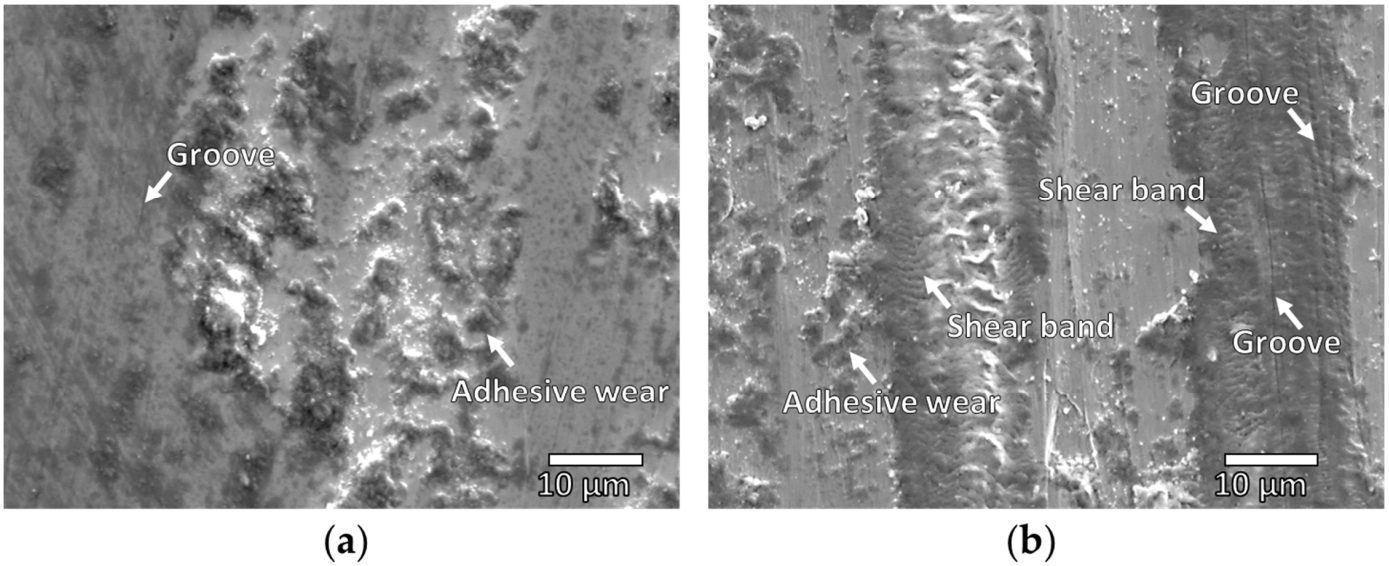

Figure 7. SEM micrographs showing adhesive wear and abrasive grooves on the wear tracks of (**a**) cold spray Inconel 713C coating and (**b**) Inconel 718 substrate.

4. Conclusions

In this study, Inconel 713C coatings were deposited on Inconel 718 substrates with high-pressure cold spray. Microstructure, hardness, and tribological properties of the Inconel 713C coatings were characterized. The main conclusions are as follows:

(1) Microstructure characterization revealed a fine grain structure and strain accumulation in the Inconel 713C coatings.
(2) Microhardness of the Inconel 713C coating was much higher than the Inconel 718 substrate. The region near the coating–substrate interface showed a higher hardness than the coating surface due to the peening effect from non-deposited particles.
(3) Wear resistance of the Inconel 718 substrate can be improved threefold with a cold-sprayed Inconel 713C coating serving as a protective layer.
(4) The main wear mechanisms of the Inconel 713C coatings are oxidation, tribo-film formation, and adhesion wear.

Author Contributions: Conceptualization, K.W., W.S. and A.W.-Y.T.; methodology, K.W., W.S. and A.W.-Y.T.; validation, K.W. and S.W.C.; formal analysis and investigation, K.W., S.W.C. and W.Z.; data curation, K.W. and S.W.C.; writing—original draft preparation, K.W.; writing—review and editing, W.Z. and S.C.T.; visualization, K.W.; supervision, W.Z. and E.L.; project administration, W.Z.; funding acquisition, W.Z., E.L. and S.C.T. All authors have read and agreed to the published version of the manuscript.

Funding: This research was funded by the National Research Foundation of Singapore, Rolls-Royce Singapore Pte Ltd., and Nanyang Technological University through grant numbers 002123-00002 and 002124-00002.

Institutional Review Board Statement: Not applicable.

Informed Consent Statement: Not applicable.

Data Availability Statement: Not applicable.

Acknowledgments: This study is supported under the RIE2020 Industry Alignment Fund—Industry Collaboration Projects (IAF-ICP) Funding Initiative, as well as cash and in-kind contribution from Rolls-Royce Singapore Pte Ltd.

Conflicts of Interest: The authors declare no conflict of interest.

References

1. Laskowski, J.A.; Dellacorte, C. *Friction and Wear Characteristics of Candidate Foil Bearing Materials from 25 °C to 800 °C*; National Aeronautics and Space Administration: Washington, DC, USA, 1996.
2. Lachowicz, M.; Dudziński, W.; Haimann, K.; Podrez-Radziszewska, M. Microstructure transformations and cracking in the matrix of γ-γ′ superalloy Inconel 713C melted with electron beam. *Mater. Sci. Eng. A* **2008**, *479*, 269–276. [CrossRef]
3. Keshavarz, M.K.; Turenne, S.; Bonakdar, A. Solidification behavior of inconel 713LC gas turbine blades during electron beam welding. *J. Manuf. Process.* **2018**, *31*, 232–239. [CrossRef]
4. Lachowicz, M.; Dudziński, W.; Podrez-Radziszewska, M. TEM observation of the heat-affected zone in electron beam welded superalloy Inconel 713C. *Mater. Charact.* **2008**, *59*, 560–566. [CrossRef]
5. Assadi, H.; Gärtner, F.; Stoltenhoff, T.; Kreye, H. Bonding mechanism in cold gas spraying. *Acta Mater.* **2003**, *51*, 4379–4394. [CrossRef]
6. Sun, W.; Tan, A.W.Y.; Marinescu, I.; Toh, W.Q.; Liu, E. Adhesion, tribological and corrosion properties of cold-sprayed CoCrMo and Ti6Al4V coatings on 6061-T651 Al alloy. *Surf. Coat. Technol.* **2017**, *326*, 291–298. [CrossRef]
7. Wu, K.; Chee, S.W.; Sun, W.; Tan, A.W.-Y.; Tan, S.C.; Zhou, W. Cold Spray Coatings for Surface Enhancement of Inconel 718. In Proceedings of the 2nd International Conference on Advanced Surface Enhancement (INCASE 2021), Singapore, 7–8 September 2021; Wei, Y., Chng, S., Eds.; Springer: Berlin/Heidelberg, Germany, 2021; pp. 159–162.
8. ASTM. *E2109-01—Standard Test Methods for Determining Area Percentage Porosity in Thermal Sprayed Coatings*; ASTM International: West Conshohocken, PA, USA, 2017. [CrossRef]
9. ASTM. *G99-17: Standard Test Method for Wear Testing with a Pin-on-Disk Apparatus G99-17*; ASTM International: West Conshohocken, PA, USA, 2017. [CrossRef]
10. Wu, K.; Sun, W.; Tan, A.W.-Y.; Marinescu, I.; Liu, E.; Zhou, W. An investigation into microstructure, tribological and mechanical properties of cold sprayed Inconel 625 coatings. *Surf. Coat. Technol.* **2021**, *424*, 127660. [CrossRef]

11. Grujicic, M.; Zhao, C.L.; DeRosset, W.S.; Helfritch, D. Adiabatic shear instability based mechanism for particles/substrate bonding in the cold-gas dynamic-spray process. *Mater. Des.* **2004**, *25*, 681–688. [CrossRef]
12. Maharjan, N.; Bhowmik, A.; Kum, C.; Hu, J.; Yang, Y.; Zhou, W. Post-Processing of Cold Sprayed Ti-6Al-4V Coatings by Mechanical Peening. *Metals* **2021**, *11*, 1038. [CrossRef]
13. Hassani-Gangaraj, M.; Veysset, D.; Champagne, V.K.; Nelson, K.A.; Schuh, C.A. Adiabatic shear instability is not necessary for adhesion in cold spray. *Acta Mater.* **2018**, *158*, 430–439. [CrossRef]
14. Goldbaum, D.; Ajaja, J.; Chromik, R.R.; Wong, W.; Yue, S.; Irissou, E.; Legoux, J.G. Mechanical behavior of Ti cold spray coatings determined by a multi-scale indentation method. *Mater. Sci. Eng. A* **2011**, *530*, 253–265. [CrossRef]
15. Tan, A.W.Y.; Sun, W.; Bhowmik, A.; Lek, J.Y.; Marinescu, I.; Li, F.; Khun, N.W.; Dong, Z.; Liu, E. Effect of coating thickness on microstructure, mechanical properties and fracture behaviour of cold sprayed Ti6Al4V coatings on Ti6Al4V substrates. *Surf. Coat. Technol.* **2018**, *349*, 303–317. [CrossRef]
16. Bhushan, B. *Introduction to Tribology*; John Wiley & Sons: Chichester, UK, 2013; ISBN 9781118403259.
17. Safarloo, S.; Loghman, F.; Azadi, M.; Azadi, M. Optimal Design Experiment of Ageing Time and Temperature in Inconel-713C Superalloy Based on Hardness Objective. *Trans. Indian Inst. Met.* **2018**, *71*, 1563–1572. [CrossRef]
18. Mahesh, B.V.; Raman, R.K.S. Role of Nanostructure in Electrochemical Corrosion and High Temperature Oxidation: A Review. *Metall. Mater. Trans. A Phys. Metall. Mater. Science* **2014**, *45*, 5799–5822. [CrossRef]
19. Tarasov, S.Y.; Kolubaev, A.V. Generation of shear bands in subsurface layers of metals in sliding. *Phys. Solid State* **2008**, *50*, 844–847. [CrossRef]
20. Vaz, R.F.; Silvello, A.; Albaladejo, V.; Sanchez, J.; Cano, I.G. Improving the wear and corrosion resistance of maraging part obtained by cold gas spray additive manufacturing. *Metals* **2021**, *11*, 1092. [CrossRef]